Broad-Band Monolithic Microwave Active Inductor and Its Application to Miniaturized Wide-Band Amplifiers

SHINJI HARA, MEMBER, IEEE, TSUNEO TOKUMITSU, MEMBER, IEEE, TOSHIAKI TANAKA, MEMBER, IEEE, AND MASAYOSHI AIKAWA, MEMBER, IEEE

Abstract—**A broad-band monolithic microwave active inductor is proposed and its characteristics are discussed. This active inductor consists of a cascode FET with a feedback resistor, and operates in a much higher frequency range than a spiral inductor. The size is independent of the inductance value. Miniaturized wide-band amplifiers in two frequency bands are also realized by utilizing the active inductors.**

I. Introduction

SPIRAL INDUCTORS are often used in MMIC designs to reduce chip size. However, this reduction is limited in wide-band MMIC's, because several spiral inductors and other inductive lines should be combined in the circuit design for a higher inductance value or, equivalently, to maintain high resonant frequencies [1]–[3]. Another limitation comes from the requirement that the spiral inductors should be separated to eliminate crosstalk. Most previously reported designs have achieved chip size reduction by neglecting the vicinity effect, as indicated by Pucel [4].

To overcome these limitations, we propose an active broad-band monolithic microwave inductor which is composed of two FET's and a feedback resistor. The most significant innovation of this active inductor is a novel circuit structure which suppresses stray capacitances to yield a much higher frequency operating range than is possible with conventional passive spiral inductors. Furthermore, this new device is small and independent of the inductance value because the inductance value is determined by the feedback resistor. Its performance compared to that of conventional spiral inductors is discussed. Active 3–7 nH inductors are fabricated and their characteristics discussed. Miniaturized wide-band amplifiers (0.1–10 GHz and 0.1–5 GHz) are also realized as the application of the active inductors, where a denser chip circuitry packing is achieved through FET-oriented configuration.

Manuscript received April 28, 1988; revised July 13, 1988.

S. Hara, T. Tokumitsu, and M. Aikawa are with ATR Optical and Radio Communications Research Laboratories, 2-1-61 Shiromi Higashi-ku, Osaka 540, Japan.

T. Tanaka was with ATR Optical and Radio Communications Research Laboratories, Osaka, Japan. He is now with the NTT Network Systems Department Center, Tokyo 100, Japan.

IEEE Log Number 8823914.

II. Configuration and Performance

A schematic of the proposed microwave active inductor is shown in Fig. 1. The active inductor is composed of a cascode FET and a feedback resistor (R_{ext}) connected between the gate of the first FET and the drain of the second FET. C_{gs1} and C_{gs2} are the FET gate–source capacitances. Since, as described below, various inductance values are obtained by changing the values of R_{ext}, the area occupied by the active inductor is independent of the inductance value.

The advantages of active inductors over spiral inductors are shown clearly in Fig. 2. The resonant frequency, which is the maximum inductor operating frequency, is compared in Fig. 2(a) to the inductance value at 1 GHz. The solid lines show the calculated characteristics of the active inductors utilizing 150 μm gate width FET's with a 20 GHz or 40 GHz cutoff frequency f_t. It is assumed here that each FET has the same C_{gs} value. The dashed line shows the calculated characteristics of the spiral inductor on 150 μm thick GaAs substrates, 300 μm $\times$ 300 μm, and a 10 μm line width, with only the line-to-line separation changed. As shown in Fig. 2(a), the operating frequency range of the active inductor is much wider than that of the spiral inductor, especially in the high inductance region. Furthermore, the operating frequency is extended as the FET's are improved.

In Fig. 2(b), the area of the active inductor and that of the spiral inductor are compared. The dots show actual spiral inductance areas reported in recent technical papers (e.g., [1] and [2]). In actual wide-band MMIC design, the larger the required inductance value, the larger the inductance area necessary. On the other hand, the area of the active inductor proposed here is consistently small and is independent of the inductance value. The crosses show the two types of fabricated active inductor areas, where the upper crosses are obtained with 150 μm gate width FET's and the lower ones with the 75 μm gate width FET's. Their areas are less than 0.15 mm^2 even at high inductance value. The area can be further reduced by using smaller gate width FET's, more compact dc bias circuitry, etc. As shown in Fig. 2(a) and (b), the proposed active inductor performs better than the spiral inductors.

In addition, area reduction from reducing the gate width

0018-9480/88/1200-1920$01.00

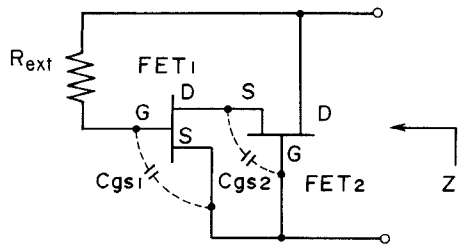

Fig. 1. Circuit configuration of the active inductor.

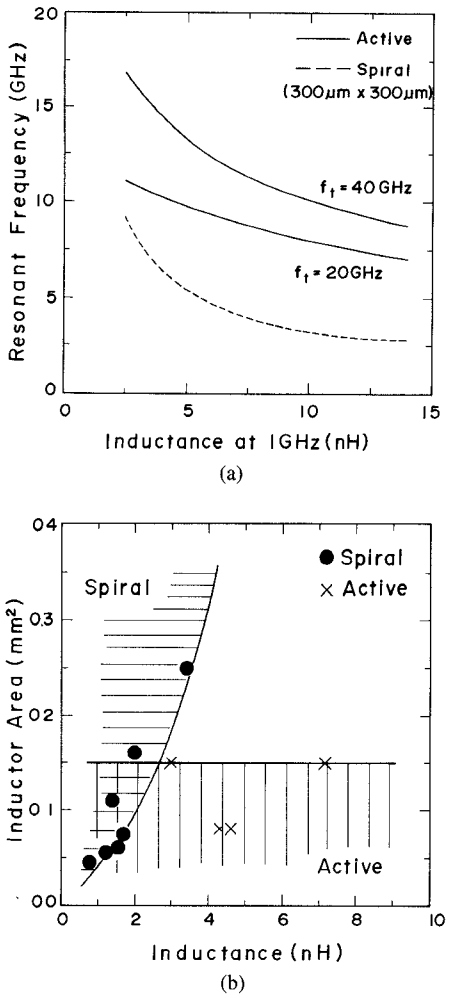

Fig. 2. Comparisons of proposed active inductor and conventional spiral inductor. (a) Resonant frequency characteristics. (b) Chip size.

also results in higher frequency operation of the active inductor, which is easily understood from the equivalent circuit shown in Fig. 4. Fig. 3 shows an example of the resonant frequency change caused by the gate width, where R_{ext} is 470 Ω and f_t of the FET's is 20 GHz. An increase of 23 percent is observed by reducing the gate width from 150 to 75 μm.

III. Maximum Operating Frequency

The broad-band characteristics of the active inductor are achieved by suppression of stray capacitances. When the FET is assumed to be a combination of the transconductance g_m and the gate-source capacitance C_{gs} only, the

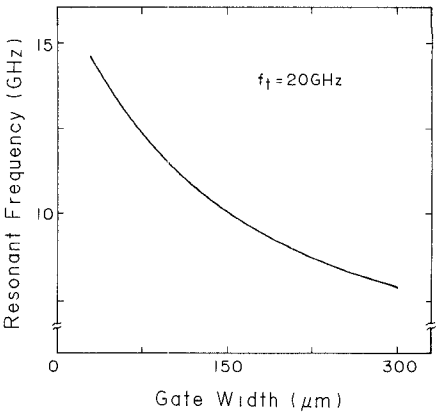

Fig. 3. Gate width versus resonant frequency of the active inductors (R_{ext} = 470 Ω).

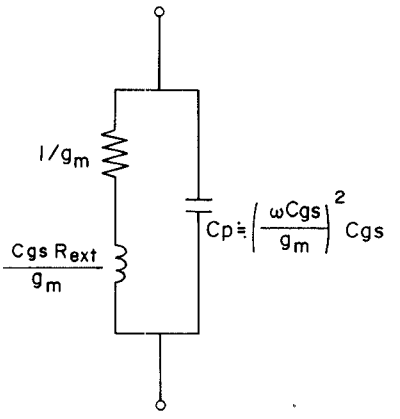

Fig. 4. Equivalent circuit of the active inductor.

impedance Z of the active inductor is expressed as follows:

$$Z = \frac{1 + j\omega C_{gs1} R_{ext}}{g_{m1} + j\omega\left[C_{gs1} - C_{gs2} + \omega^2 C_{gs2}(C_{gs1}C_{gs2}/g_{m1}g_{m2})\right]} \tag{1}$$

where the subscripts 1 and 2 correspond to, respectively, the first FET and the second FET in the cascode FET. When the cascode FET is composed of FET's with the same g_m and C_{gs}, the gate-source capacitances C_{gs1} and C_{gs2} cancel each other. Therefore, (1) is rewritten as

$$Z = \frac{1 + j\omega C_{gs} R_{ext}}{g_m + j\omega C_{gs}(\omega C_{gs}/g_m)^2}. \tag{2}$$

The typical equivalent circuit of this active inductor is shown in Fig. 4. In actual microwave FET's, $\omega C_{gs}(\omega C_{gs}/g_m)^2$ is sufficiently smaller than g_m. Thus the proposed microwave active inductor can operate in the microwave range. From (2) this active inductor can operate under the conditions presented in the following equation:

$$g_m \gg \omega C_{gs}\left(\frac{\omega C_{gs}}{g_m}\right)^2. \tag{3}$$

Equation (3) can be rewritten as (4) with the cutoff frequency f_t ($=g_m/2\pi C_{gs}$):

$$(f/f_t)^3 \ll 1. \tag{4}$$

In this equation the maximum operating frequency is about one-half of f_t.

IV. Experimental Result

A photograph of a fabricated GaAs monolithic active inductor and a circuit configuration diagram are shown in Fig. 5. Two 0.3 μm × 150 μm single-gate ion-implanted FET's with a typical cutoff frequency of 21 GHz are employed. The active inductor is located in a 400 μm × 400 μm area with dc-cut capacitors separating the dc biases for each gate.

The inductances of the active inductor obtained through one-port impedance measurements at port ①, when the other, port ②, is grounded, are shown in Fig. 6, along with the inductances of the spiral inductors calculated under the conditions of Fig. 2(a). Two kinds of active inductors are fabricated with external resistances (R_{ext}) of 320 Ω and 800 Ω, respectively. Inductances of 3.0 ± 0.4 nH and 7.7 ± 0.9 nH are obtained at frequencies ranging up to 7.6 GHz and 5.5 GHz, respectively. As shown in Fig. 6, the active inductors are at a constant inductance over a much wider frequency range than the 300 μm × 300 μm spiral inductors. With regard to the resonant frequency, some differences between the measured (Fig. 6) and calculated (Fig. 2(a)) values can be found. This degradation results from the parasitic capacitances between the dc-cut capacitors and the ground, as well as from the distribution lines connecting the inductor elements, mainly the lines existing between the first gate and second drain of the cascode FET. Therefore, it is important to minimize these capacitances and line lengths in the actual designs.

The impedance of the fabricated active inductor changes according to the gate bias voltage of the second FET, as shown in Fig. 7. This active inductor uses 75 μm gate width FET's and a 470 Ω resistor. The drain bias V_D is 5 V, the gate bias of the first FET is 0 V, and the gate bias voltage of the second FET (V_I) is changed from 0 to 2.5 V. As shown in Fig. 7, the impedance and resonant frequency can be widely varied by changing V_I. This characteristic of the active inductor is useful for MMIC characteristic tuning with no trimming.

Two-port S parameters are also measured with the results shown in Fig. 8, where the device exhibits inductive characteristics when measured from port ①, but not when measured from port ②. This difference results from the reasons mentioned above.

V. Application to Wide-Band Amplifiers

The schematic of a 0.1–10 GHz amplifier utilizing the proposed active inductors is shown in Fig. 9. A common-gate FET (CGF) with a transconductance of 20 mS is used for the input impedance match. A common-source FET (CSF) with a transconductance of 40 mS is used for the gain stage. Active inductors with low-value spiral inductors and resistors are used at the CGF and CSF output ports. The gain and the bandwidth are mainly determined by the active inductors. Element values are optimized by commercially available CAD software. A photograph of

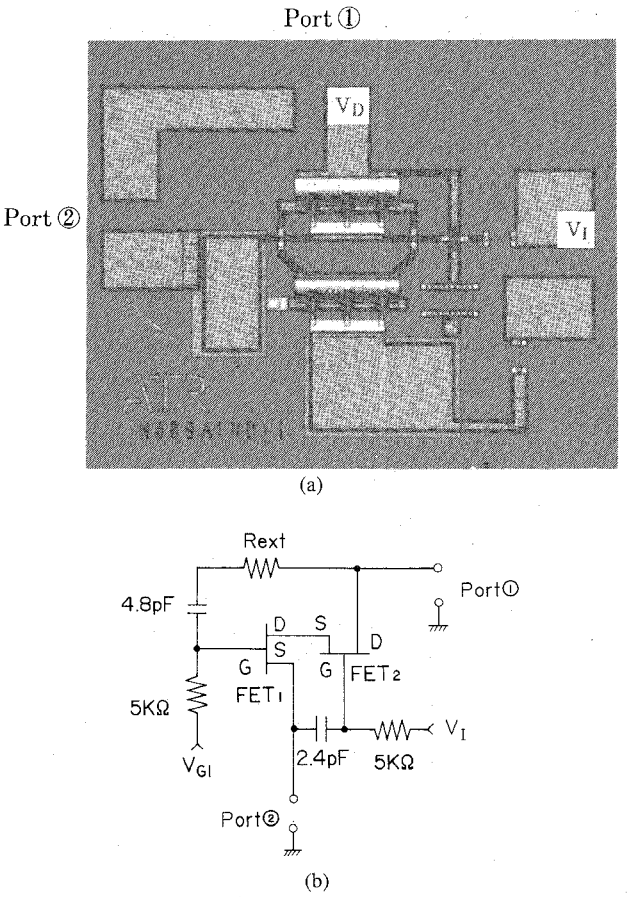

Fig. 5. The schematics of the fabricated active inductor. (a) Photograph of the chip. (b) Circuit configuration.

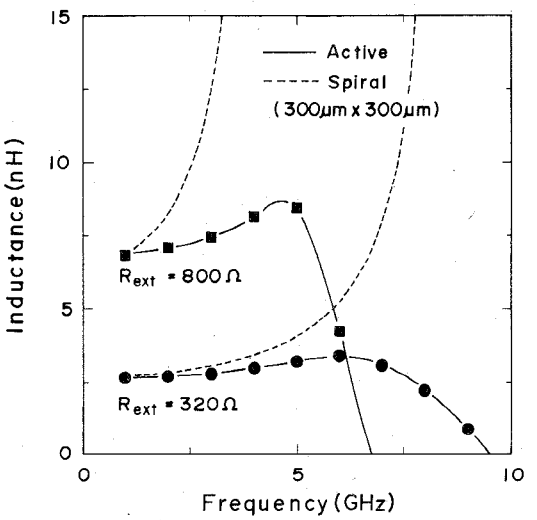

Fig. 6. Inductance–frequency characteristics of the fabricated active inductors along with calculated inductances of the spiral inductors.

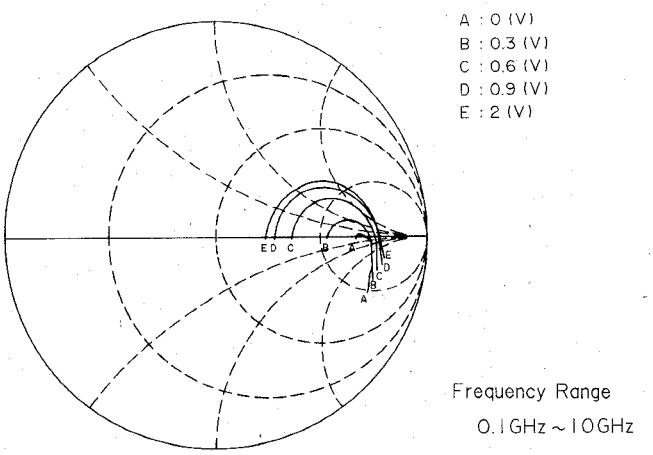

Fig. 7. Active inductor impedance versus frequency at various gate biases (W_g = 75 μm, R_{ext} = 470 Ω).

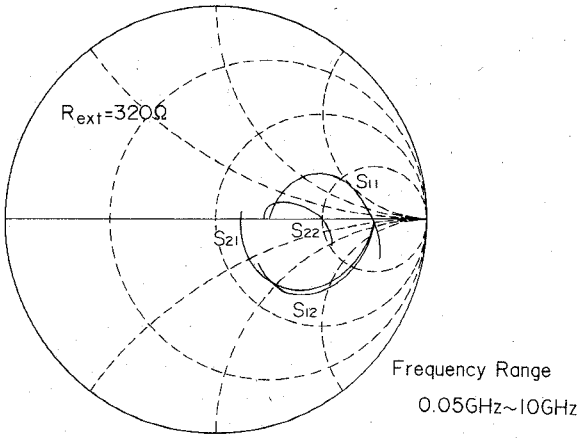

Fig. 8. *S* parameters of the fabricated active inductor (two-port measurement).

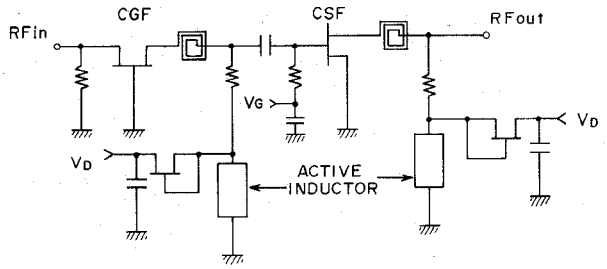

Fig. 9. Circuit configuration of active matching amplifier using active inductor (0.1–10 GHz).

a fabricated MMIC amplifier is shown in Fig. 10. Eight 0.5 μm gate length FET's obtained through epitaxial growth are used in this amplifier. The two active inductors consist of a pair of 75 μm gate width FET's and R_{ext} has values of 430 Ω and 470 Ω, respectively. Two FET's which have a 150 μm gate width are used for supplying dc bias. The input CGF gate width is 150 μm and the output CSF gate width is 300 μm. The total chip size is only 1.0 mm × 1.3 mm × 0.6 mm. Measured and predicted performance agree closely, as shown in Fig. 11, where 6 dB gain, input *VSWR* less than 2, output *VSWR* less than 2.4, and isolation greater than 35 dB are obtained in the frequency range from 0.1 to 9 GHz.

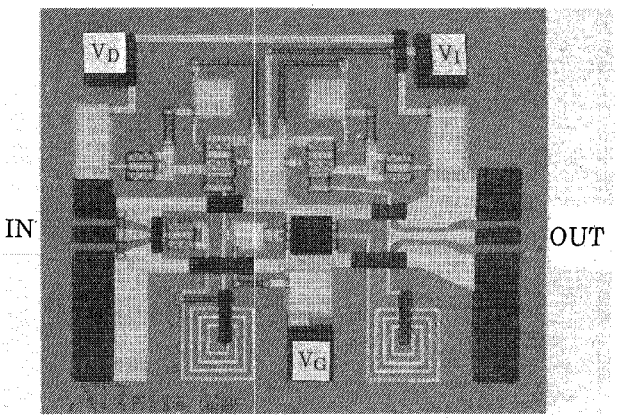

Fig. 10. Photograph of active matching amplifier (0.1–10 GHz).

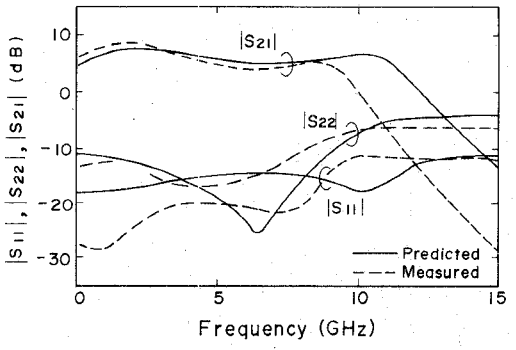

Fig. 11. Performance of fabricated 0.1–10 GHz amplifier.

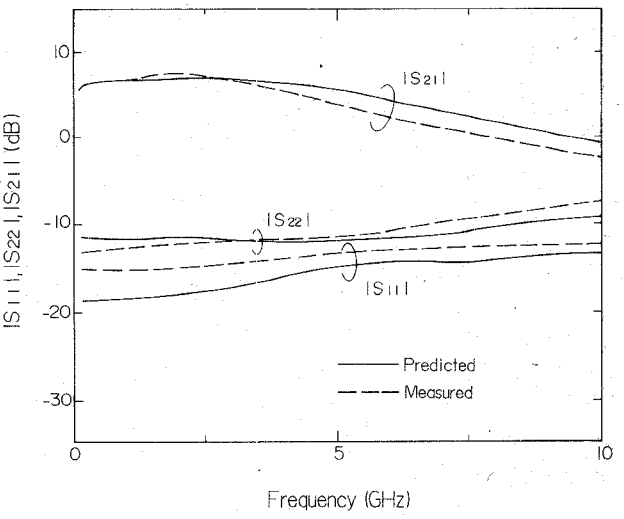

Fig. 12. Performance of fabricated 0.1–5 GHz amplifier.

A 0.1–5 GHz amplifier is also fabricated by directly connecting the terminals of the series spiral inductors in Fig. 9. The measured and predicted performance values are shown in Fig. 12, where 7 dB gain, input *VSWR* less than 1.5, output *VSWR* less than 1.7, and isolation greater than 45 dB are obtained in the frequency range from 0.1 to 4.5 GHz.

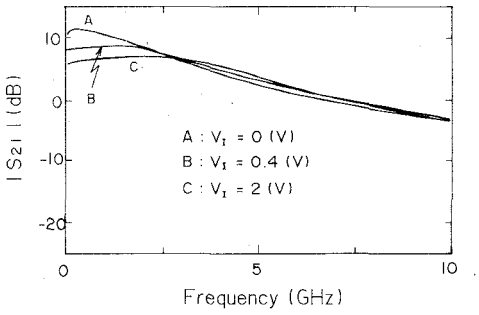

Fig. 13. Tunable gain characteristics by the gate bias V_I.

Fig. 13 shows an example of gain–frequency characteristic change in the 0.1–5 GHz amplifier according to the gate bias voltage V_I. From this figure, it is seen that an effective gain-slope adjustment can be achieved with no trimming.

VI. Conclusions

A broad-band microwave active inductor has been proposed. This active inductor consists of a cascode FET with a feedback resistor and has the following features:

1) very high frequency operation
2) small size independent of the inductance value.

These have been demonstrated through analysis and/or simulations. Several active inductors have been fabricated and tested. The experimental results showed that the active inductors are greatly superior to the spiral inductors in miniaturized and wide-band MMIC's. Miniaturized wide-band amplifiers with FET-oriented configuration have also been fabricated, and good performance was achieved. This active inductor should prove valuable in designing smaller and more efficient MMIC's.

Acknowledgment

The authors would like to thank Dr. K. Habara of Advanced Telecommunications Research (ATR) Institute International and Dr. Y. Furuhama of ATR Optical and Radio Communications Research Laboratories for their helpful discussions and valuable suggestions throughout this work.

References

[1] K. P. Weller *et al.*, "GaAs monolithic lumped element multistage microwave amplifier," in *1983 IEEE MTT-S Int. Microwave Symp. Dig.*, pp. 69–73.

[2] B. Maoz *et al.*, "A fully-integrated, 0.5 watt, 2 to 6 GHz MMIC amplifier," in *Proc. 16th European Microwave Conf.*, 1986, pp. 261–265.

[3] J. G. Tenedorio, "Availability of mature GaAs MMIC products and services increases system capability," *Monolithic Technol.*, pp. 40–43, Oct. 1987.

[4] R. A. Pucel, "MMIC's modeling, and CAD—Where do we go from here?" in *Proc. 16th European Microwave Conf.*, 1986, pp. 61–70.

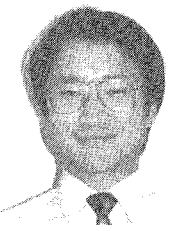

Shinji Hara (M'88) was born in Toyama, Japan, in 1960. He received the B.E. (1982) and M.E. (1984) degrees in electrical engineering from Waseda University, Tokyo, Japan.

In 1984, he joined the Tokyo Research Laboratories of the Sharp Corporation, Chiba, Japan. Since September 1986 he has been a researcher at ATR Optical and Radio Communications Research Laboratories, Osaka, Japan, on leave from the Sharp Corporation. At ATR, he has been engaged in research on circuit design technology to realize highly integrated MMIC's.

Mr. Hara is a member of the Japan Society of Applied Physics and the Institute of Electronics, Information and Communication Engineers of Japan.

*

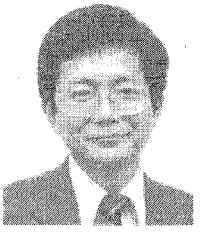

Tsuneo Tokumitsu (M'88) was born in Hiroshima, Japan, in 1952. He received the B.S. and M.S. degrees in electrical engineering from Hiroshima University, Hiroshima, in 1974 and 1976, respectively.

He joined the Yokosuka Electrical Communication Laboratories, Nippon Telegraph and Telephone Public Corporation, Yokosuka, in 1976, where he did research on microwave and millimeter-wave integrated circuits, MIC's, and MMIC's and worked on the development of on-board satellite equipment. In September 1986 he joined ATR Optical and Radio Communications Research Laboratories, Osaka, where he is currently engaged in research on highly integrated MMIC's for future digital mobile communications.

Mr. Tokumitsu is a member of the Institute of Electronics, Information and Communication Engineers of Japan.

*

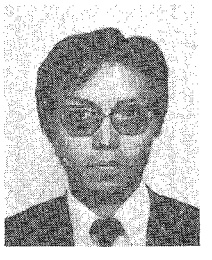

Toshiaki Tanaka (M'87) was born in Osaka, Japan, on May 23, 1951. He received the B.S. and M.S. degrees in communication engineering from Osaka University, Osaka, Japan, in 1975 and 1977, respectively.

In 1977, he joined the NTT ECL Systems, Yokosuka, Kanagawa-ken, Japan, where he worked on on-board equipment for satellite communications systems. From 1986 to 1988, he was with the Advanced Telecommunications Research Institute International (ATR), Osaka, Japan, where he was engaged in research and development of microwave passive components and GaAs monolithic microwave integrated circuits (MMIC's). In 1988 he was appointed Executive Engineer of the NTT Network Systems Development Center, Tokyo, Japan. Since then he has been engaged in the development of integrated networks.

Mr. Tanaka is a member of the Institute of Electronics, Information and Communication Engineers (IEICE) of Japan.

*

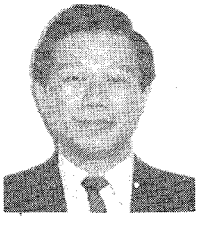

Masayoshi Aikawa (M'78) was born in Saga, Japan, on October 16, 1946. He received the B.S., M.S., and Ph.D. degrees in electronics engineering from Kyushu University, Fukuoka, Japan, in 1969, 1971, and 1985, respectively.

In 1971 he joined the Musashino Electrical Communication Laboratories, Nippon Telegraph and Telephone Public Corporation, Tokyo, Japan, where he did research and development work on microwave and millimeter-wave integrated circuits, MIC's, MMIC's, and equipment for 20 GHz digital radio trunk transmission systems and 26 GHz subscriber radio systems. In 1986, he joined ATR Optical and Radio Communications Research Laboratories, Osaka, Japan, where he is currently engaged in research on basic techniques for future mobile communication systems.

Dr. Aikawa is a member of the Institute of Electronics, Information and Communication Engineers of Japan.